www.czasopisma.pan.pl PAN POLSKA AKADEMIA NAUK www.journals.pan.pl

Arch. Metall. Mater. **65** (2020), 2, 761-765

DOI: 10.24425/amm.2020.132817

W. MATYSIAK[1], T. TAŃSKI[1], W. SMOK[1*], O. POLISHCHUK[2]

THIN SnO_2 FILMS MANUFACTURED VIA THE SOL-GEL AND ELECTROSPINNING METHODS

The aim of this work was to produce a thin SnO_2 film by a technique combining the sol-gel method and electrospinning from a solution based on polyvinylpyrrolidone and a tin chloride pentahydrate as a precursor. The spinning solution was subjected to an electrospinning process, and then the obtained nanofiber mats were calcined for 10 h at 500°C. Then, the scanning electron microscopy morphology analysis and chemical composition analysis by X-ray microanalysis of the manufactured thin film was performed. It was shown that an amorphous-crystalline layer formed by the SnO_2 nanofiber network was obtained. Based on the UV-Vis spectrum, the width of the energy gap of the obtained layer was determined.

Keywords: thin films; nanofibers; tin oxide; electrospinning; optical properties

1. Introduction

Recently, there has been a great interest in an area of the thin films based semiconductor metal oxides, which unique optical properties create wide possibilities of their application in many industries as elements of sensors, lithium-ion batteries or modern photovoltaic cells [1-4]. In addition to such oxides as ZnO, TiO_2, CuO or Bi_2O_3, also SnO_2 presents interesting optical and sensory properties [5-9]. This material is a semiconductor with high chemical stability, good mechanical properties, high temperature resistance and high optical transparency in the visible range of the electromagnetic spectrum [10-12]. The optoelectronic properties of SnO_2 nanostructures are highly influenced by the synthesis method, which defines their structure and morphology, as well as the amount of impurities. Table 1 shows the relationship between the value of the energy gap width and the method of preparation thin tin oxide films [13-18]. It can be seen that the preparing method determine the structure and optical band gap of the material in a large range. It can be noticed that the value of the energy gap obtained by us is more similar to the amorphous than crystalline layer, which results from the higher of this phase. Manufacturing methods of this type of material include chemical and physical vapor deposition, magnetron sputtering or laser ablation, however, due to the simplicity and cost-effectiveness of combining the sol-gel method with electrospinning technique is currently widely investigated [19-22]. In the first stage of this method, thin nanofiber mats are produced in the electrospinning process from a suitably prepared solution containing polymer, precursor and solvents, then the as obtained nanofibrous mats are heat treated to remove the polymer matrix, which leads to producing final thin films [23]. The first literature reports on the production of thin layers of SnO_2 using a sol gel technique and electrospinning appeared in 2006, when a scientific team led by N. Dharmaraj presented the results of their work on the analysis of the effect of calcination temperature on the structure and morphology of SnO_2 nanofibers [24]. For this purpose, using a solution based on poly(vinyl alcohol) (PVA) and the precursor $SnCl_2{\cdot}2H_2O$, electrospinning of composite nanofibers PVA/$SnCl_2$ was performed. Then obtained materials were subjected to the thermal treatment by heating at various temperatures: 300, 400, 500 and 600°C. The morphology and structure analysis carried out using the scanning electron microscope (SEM) and the Fourier-Transform Infrared Spectroscopy (FTIR) showed that temperatures below 600°C did not allow complete polymer degradation and fully crystalline SnO_2 fibers were obtained only after calcination at 600°C. In 2008, Y. Zhang et al. also produced crystalline SnO_2 nanofibers using tin chloride pentahydrate ($SnCl_4{\cdot}5H_2O$) as a precursor [25]. After the electrospinning process with variable parameters: distance and voltage between the electrodes of 0.5-2.6 cm and 5-10 kV, PVA/$SnCl_4$ nanofibers were calcined at the following temperatures: 300, 500 and 700°C for 4 hours. A SnO_2 nanofibers produced in this way

[1] SILESIAN UNIVERSITY OF TECHNOLOGY, DEPARTMENT OF ENGINEERING MATERIALS AND BIOMATERIALS, 18A KONARSKIEGO STR., 44-100 GLIWICE, POLAND
[2] KHMELNYTSKYI NATIONAL UNIVERSITY, DEPARTMENT OF MACHINES AND APPARATUS, ELECTROMECHANICAL AND POWER SYSTEMS, KHMELNYTSKYI, UKRAINE

* Corresponding author: weronika.smok@polsl.pl

were used to construct a gas sensor and its sensory properties were investigated. The analysis showed that high sensitivity, short response time and good reproducibility were obtained by using thin nanofibrous films of SnO_2. An international team from South Korea and India in 2011 published the results of their work, in which they showed that the temperature and calcination time of nanofibers produced by electrospinning from a solution of PVA/DMF/EtOH/$SnCl_2 \cdot 2H_2O$ have a significant impact on the size of the nanofibers grain [26]. Composite PVA/SnO_2 fibers were prepared with the following process parameters: 20 kV potential difference between the electrodes, 20 cm distance between the electrodes and 0.03 ml/h solution feed rate. Then, some of the samples were soaked at the same time of 6 hours, but at different temperatures in the range of 500-900°C, while some at the same temperature of 600°C, but for a different period of time from 4-24 hours. SEM analysis of the fibers after calcination has shown that as the temperature and calcination time increase, the grain diameter of SnO_2 nanofibers increases. In addition, analysis of the ability to detect CO and NO_2 showed that sensors from fine-grained nanofibers have significantly better sensory properties than large-grain nanofibers. L. Cheng and colleagues showed that ethanol sensors built of coreless, porous SnO_2 nanofibers formed as a result of electrospinning and calcination are characterized by fast response and high sensitivity to ethanol at 300°C [27]. The PVP/DMF/EtOH/$SnCl_2 \cdot 2H_2O$ solution was subjected to electrospinning (no data on the applied process parameters), then immediately after spinning process, the nanofibers were calcined at 600°C for 2 hours, thanks to which polycrystalline nanofibers with an average diameter of approx. 200 nm and thickness of the wall of 20-30 nm were obtained, which rough surface was agglomerated tin oxide nanoparticles with a size of about 20 nm. Very good sensory properties were observed by preparing a paste from nanofibers and deionized water, which was placed in a ceramic tube and contacted with ethanol, acetone, ammonia, methanol and acetic acid in gaseous form. The authors of the study claimed that the favorable sensory properties, especially when detecting ethanol, could be attributed to the lack of core and porosity of nanostructures.

TABLE 1

The energy band gap value of thin SnO_2 films synthesized by various methods

Materials type	Strcture	Synthesis method	Band gap [eV]	Ref.
Thin films	Amorphous	Atomic Layer deposition (ALD)	3.75	13
Thin films	Tetragonal rutile	Spray pyrolysis	3.96-3.99	14
Thin films	Tetragonal rutile	Spray pyrolysis	4.64	15
Thin films	Tetragonal rutile	Radio frequency sputtering	2.85-3.39	16
Nanofibrous films	Tetragonal rutile	Sol gel and electrospinning	3.48	17
Nanofibrous films	Tetragonal rutile	Sol gel and electrospinning	3.59	18
Nanofibrous films	Amorphous/ rutile	Sol gel and electrospinning	3.78	This work

The purpose of this work was to produce a polymer/precursor composite nanofibrous film via electrospinning from a solution of and calcining at high temperature to obtain a ceramic thin film of SnO_2. The morphology and optical properties analysis of manufactured nanomaterial proved that there is a possibility of using this type of materials in modern dye cells (DSSC).

2. Materials and methods

In order to prepare the spinning solutions, the following reagents were used: poly(vinylpyrrolidone) (PVP purity of 99%, Mw = 1,300,000 g/mol), ethanol (EtOH, purity 99.8%), N, N-dimethylformamide (DMF, purity of 99,8%) and tin (IV) chloride pentahydrate ($SnCl_4 \cdot 5H_2O$, purity of 98%) (all purchased from Sigma-Aldrich).

In the first step, by adding PVP to mixture of EtOH and DMF (1:1 mass ratio) in an amount corresponding to 8% wt. relative to the total weight of solvents and stirring for 48 h, a polymer solution was prepared. Then, a certain amount of tin oxide precursor was dissolved in polymer solution and after 48 h of stirring, the homogenous solution containing PVP:$SnCl_4 \cdot 5H_2O$ in mass ratio of 1:1 was obtained. The spinning solution was directly put into plastic syringe pump. The composite PVP/$SnCl_4$ nanofibrous film was prepared using FLOW – Nanotechnology Solutions Electrospinner 2.2.0-500 device with following parameters: voltage and distance between electrodes of 22 kV and 15 cm and a flow rate of 0,4 ml/h. Then, the as obtained nanofibers were calcinated in a vacuum furnace HT-2100-G-Vac-Graphit-Special at 500°C temperature for 10 hours with the heating rate 10°C/min to remove the polymer matrix.

To provide the morphology and chemical composition of the obtained materials, the Zeiss Supra 35 scanning electron microscope (SEM) with the EDAX Trident XM4 series x-ray spectrometer (EDX) were used. Based on the SEM images, a hundred-fold measurements of the diameters of the randomly selected composite and hybrid nanofibers were performed using the Digital Micrograph. The Fourier-Transform Infrared Spectroscopy (FTIR) spectra of prepared nanomaterials were carried out by spectrophotometer FTIR Nicolet 6700/8700. In order to determine the optical properties of manufactured thin SnO_2 films, the absorbance measurements have been carried out using the spectrophotometer UV-VIS Evolution 220 by Thermo-Scientific Company.ph software. Moreover, on the basis of UV-VIS absorption measurement, the optical energy band gap was calculated.

3. Results and discussion

3.1. Morphology and structure analysis

Figure 1a shows SEM image of PVP/SnO_2 composite nanofibers obtained directly after the electrospinning process.

It was observed that the produced nanofiber mat consisted of chaotically arranged, smooth nanofibers. The nanofibers were characterized by the lack of structural defects, the constant diameter over the entire length of the fiber, which average value was equal to 76 nm, and the most numerous group were nanofibers with a diameter in the range of 65-75 nm. The SEM image of material after calcination shown in Fig. 1b confirms, that as a result of calcining PVP/SnO_2 nanomat, a thin film made of network-like SnO_2 nanofibers was obtained. In contrast to surface topography of nanofibers before calcination, the SnO_2 nanostructures have a highly developed surface with numerous protuberances, which are tin oxide crystallites. In addition, after calcination, a decrease in average diameter to 51 nm was observed, with 25% of nanofibers having a diameter in the range of

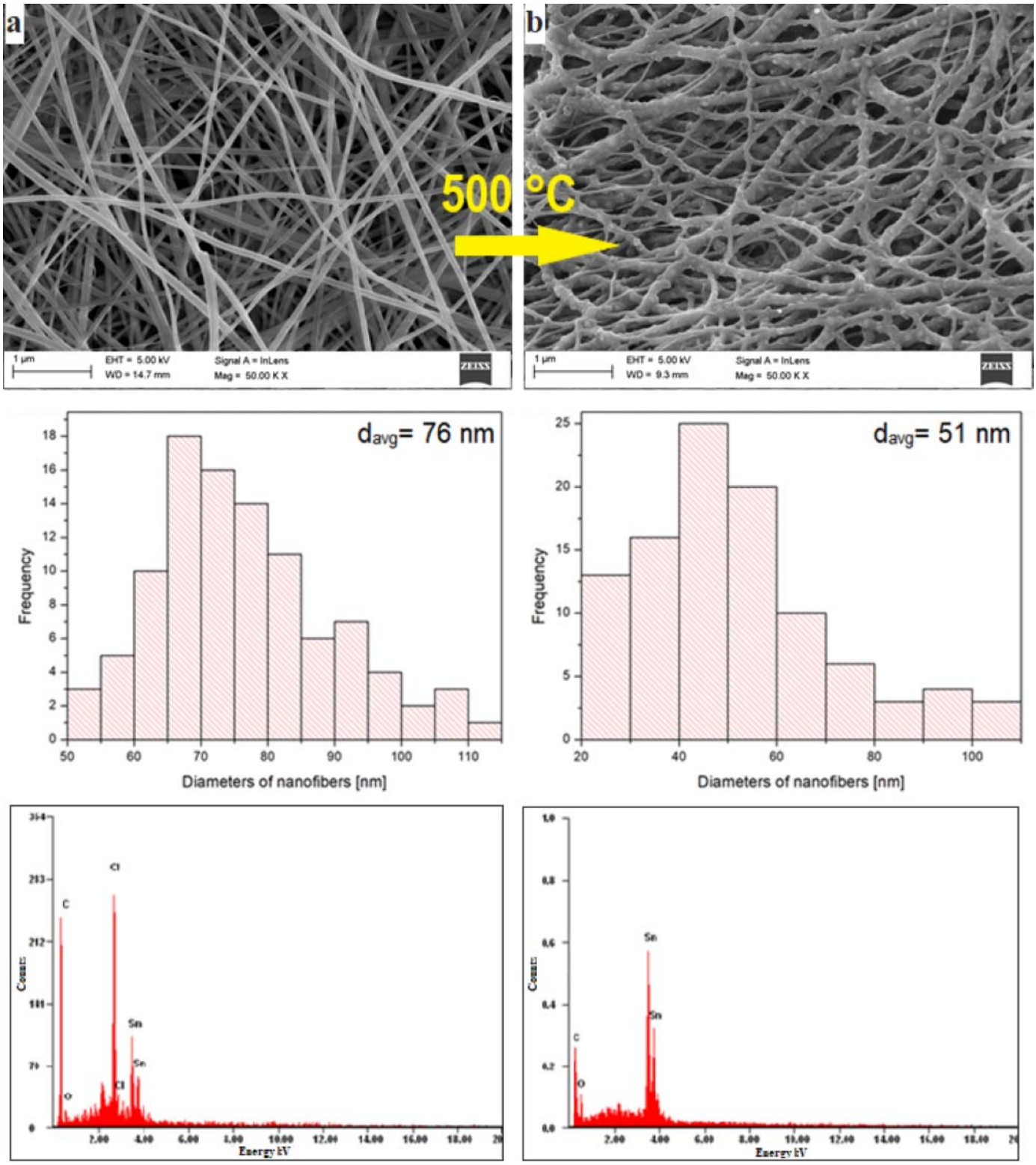

Fig. 1. SEM images with histograms showing the distribution hundred-fold measurements of diameters of randomly chosen fibers and EDX spectra of: a) composite PVP/$SnCl_4$ thin film directly after electrospinning, b) ceramic SnO_2 thin film after calcination process

40-50 nm. The decrease in diameter was caused by the degradation of the polymer matrix during high temperature calcination. The analysis of the chemical composition performed with use of EDX for the sample before calcination showed the presence of precursor elements – Sn and Cl, while the EDX spectrum of the sample after heat treatment, on which Sn is the mainly observed element, confirms the removal of polymers and obtaining the ceramic nanomaterial SnO_2 (the peak marked as carbon comes from carbon tape used for the test).

The FTIR spectra of obtained composite PVP/$SnCl_4$ and ceramic SnO_2 nanofibers are presented in Fig 2. In the spectra recorded for mats before calcination, the strong peak is observed at 2958 cm^{-1}, it can be assigned to the asymmetric stretching vibration of C-H bending of PVP. The peaks around 1635 and 1466 cm^{-1} are due to the vibration of the carbonyl group C=O and O-H bending, respectively. The -C-N stretching due to PVP presence can be observed around 1261 cm^{-1}. The spectrum of PVP/$SnCl_4$ nanofibers showed the characteristic broad absorption band of O-H bond around 3400 cm^{-1}. It can be seen that there is a wide band located at 524-720 cm^{-1} which corresponds to the –Sn-O bond [24,27]. In the spectrum of the material after calcination, only one characteristic band is visible at position 625-710 cm^{-1}, which results from the presence of a fundamental Sn-O bond. The absence of peaks characteristic of PVP confirms a polymer degradation [24].

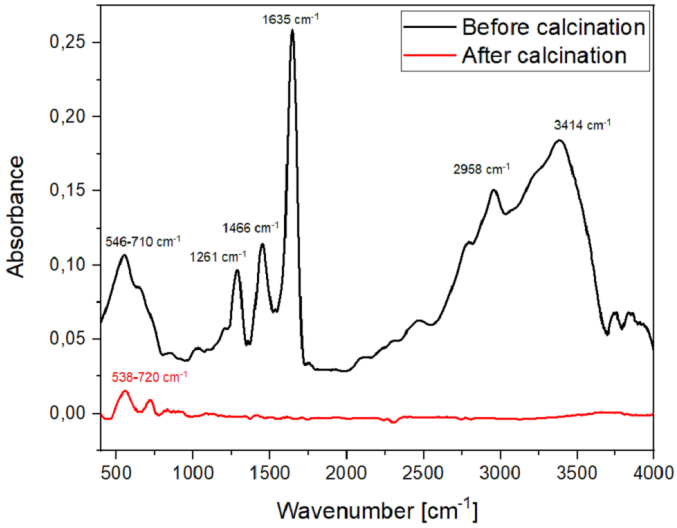

Fig. 2. FTIR spectra of a) composite PVP/$SnCl_4$ thin film, b) ceramic SnO_2 thin film

3.2. Optical properties analysis

The optical properties of SnO_2 thin film was investigated by employing UV-vis spectroscopy. The figure 3 presents room temperature optical absorption spectra in the range of 200-1100 nm. SnO_2 nanofibers exhibited strong absorbance with broad absorption edge below 302 nm and gradual fall in absorption in the UV region, whereas low absorbance is found in visible region, which agrees with the results obtained so far [13-18].

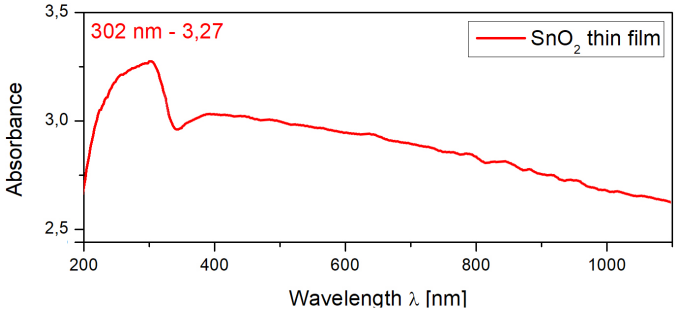

Fig. 3. Spectra of absorbance as a function of the wavelength of electromagnetic radiation recorded to the obtained thin SnO_2 film

Optical energy band gap E_g for obtained SnO_2 thin film was estimated based on the plots of $(\alpha h\upsilon)^2$ versus photon energy '$h\upsilon$', as depicted in figure 4, using Tauc's equation [28, 29]:

$$\alpha h\upsilon = A(h\upsilon - E_g)^n \quad (1)$$

where, α – absorption coefficient, h – Planck constant, υ – electromagnetic radiation frequency, A – constant, E_g – energy band gap, n – transition probability (n = 1/2 for materials with direct interband transitions)

The value of the energy gap of the obtained thin SnO_2 film was 3.78 eV, which is close to the thin layers made of this material and this proves that this type of material has great potential for photovoltaic applications and in optoelectronic devices [13-18].

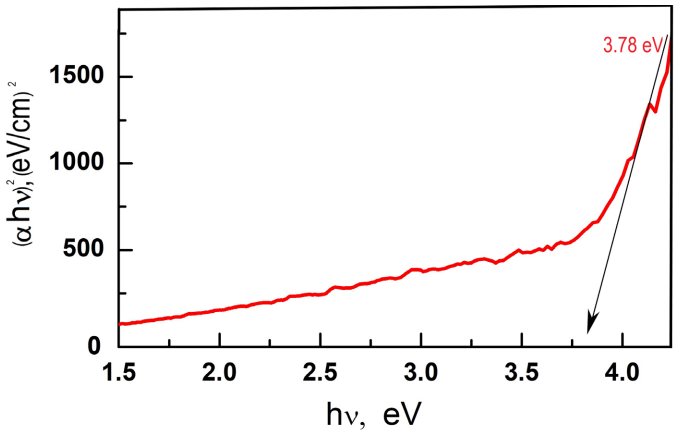

Fig. 4. Formula $(\alpha h\upsilon)^2$ as a function of the quantum radiation energy with matching straight lines, indicating the value of energy gaps of the studied thin SnO_2 film

4. Conclusion

The aim of this work was to produce a thin ceramic SnO_2 film by combining the sol-gel method and electrospinning from a solution PVP/$SnCl_4$/DMF/EtOH and investigate its morphology, structure and optical properties. At first, spinning solution was prepared by adding $SnCl_4$ precursor to PVP solution, then prepared homogenous solution was electrospuned to obtain thin fibrous composite polymer/precursor mat. As obtained mat was calcined in 500°C for 10 h to decompose the organic matrix and obtain pristine SnO_2 thin film. The carried-out SEM analysis

showed that as a result of the heat treatment of the smooth nanofiber mat, a thin film with the SnO_2 rough nanofiber network structure was produced. An analysis of the optical properties of ceramic thin layer revealed a high absorption of electromagnetic radiation of the UV range. Moreover, based on $(\alpha hv)^2$ as a function of the quantum radiation energy formula, the value of the energy gap was determined which was 3.78 eV. The results suggest that due to the favorable optical properties, the manufactured thin film can be applied in photovoltaics as novel type solar cells and optoelectronic devices.

Acknowledgements

The research presented in this paper was financed by the National Science Centre, Poland based on the decision number 2016/23/B/ST8/02045.

REFERENCES

[1] C. Lu, Z. Chen, Int. J. Hydrog. Energia. **35** (22), 12561-12567 (2010).
[2] C.Y. Tsay, K.C. Pai, Thin Solid Films **654**, 11-15 (2018).
[3] B. Zhao, F. Mattelaer, J. Kint, A. Werbrouck, L. Henderick, M. Minjauw, C. Detavernier, Electrochim. Acta **320**, 134604 (2019).
[4] K.S. Anuratha, H.S. Peng, Y. Xiao, T.C. Wei, J.Y. Lin, Electrochim. Acta **295**, 662-667 (2019).
[5] C.D. Lokhande, D.P. Dubal, O.S. Joo, Curr. Appl Phys. **11** (3), 255-270 (2011).
[6] Q. Wang, X. Li, W.M. Zhao, S. Jin, Appl. Surf. Sci. (2019).
[7] X.H. Shi, K.J. Xu, Mater. Sci. Semicond. Process **58**, 1-7 (2017).
[8] I.M. El Radaf, T.A. Hameed, T.M. Dahy, Ceram. Int. **45** (3), 3072-3080 (2019).
[9] M.J. Mortelliti, A.N. Wang, J.L. Dempsey, Polyhedron **171**, 433-447 (2019).
[10] J.C. Manifacier, M. De Murcia, J.P. Fillard, E. Vicario, Thin Solid Films. **41**, 127-144 (1977).
[11] T.M. Al-Saadi, B.H. Hussein, A.B. Hasan, A.A. Shehab, Energy Procedia. **157**, 457-465 (2019).
[12] H. Hartnagel, (Eds.), Semiconducting transparent thin films, CRC Press (1995).
[13] J.H. Bang, M. Lee, A. Mirzaei, M.S. Choi, H.G. Na, C. Jin, Y. Choi, Ceram. Int. **45** (6), 7723-7729 (2019).
[14] S.P. Choudhury, S.D. Gunjal, N. Kumari, K.D. Diwate, K.C. Mohite, A. Bhattacharjee, Mater. Today: Proc. **3** (6), 1609-1619 (2016).
[15] P.M. Mwathe, R. Musembi, M. Munji, B. Odari, L. Munguti, A.A. Ntilakigwa, B. Muthoka, Int. J. Mater. Sci. App. **3** (5), 137-142 (2014).
[16] S. Baco, A. Chik, F.M. Yassin, J. Sci. Tech. **4**(1) (2012).
[17] Z.H. Bakr, Q. Wali, J. Ismai, N.K. Elumalai, A. Uddin, R. Jose, Electrochim. Acta **263**, 524-532 (2018).
[18] K. Wang, Z. Qian, Z. Guo, Mater. Res. Bull. **111**, 202-211 (2019).
[19] S. Das, V. Jayaraman, Prog. Mater. Sci. **66**, 112-255 (2014).
[20] Z. Lounis, M.H. Bouslama, C. Zegadi, D. Ghaffor, A. Baizid, M.S. Halati, A. Ouerdane, J. Electron. Spectrosc. **226**, 9-16 (2018).
[21] W. Matysiak, T. Tański, W. Smok, Sol. St. Phen. **293**, 35-49 (2019).
[22] R.D. Vispute, V.P. Godbole, S.M. Chaudhari, S.M. Kanetkar, S.B. Ogale, J. Mater. Res. **3** (6), 1180-1186 (1988).
[23] Z. Li, C. Wang, One-dimensional nanostructures: electrospinning technique and unique nanofibers. Heidelberg/New York/ Dordrecht/London: Springer (2013).
[24] N. Dharmaraj, C.H. Kim, K.W. Kim, H.Y. Kim, E.K. Suh, Spectrochim. Acta Part A. **64** (1), 136-140 (2006).
[25] Y. Zhang, X. He, J. Li, Z. Miao, F. Huang, Sensor. Actuat. B-Chem. **132** (1), 67-73 (2008).
[26] Y.J. Park, K. Asokan, S. W. Choi, S. S. Kim, Sensor. Actuat. B-Chem. **152** (2), 254-260 (2011).
[27] S.I. Boyadjiev, O. Kéri, P. Bárdos, T. Firkala, F. Gáber, Z.K. Nagy, I.M. Szilágyi, App. Surf. Sci. **424**, 190-197 (2017).
[28] J. Tauc, R. Grigorovici, A. Vancu, Phys. Status Solidi B. **15** (2), 627-637 (1966).
[29] W. Matysiak, T. Tański, App. Surf. Sci. **474**, 232-242 (2019).
[30] T. Tański, W. Matysiak, B. Hajduk, Beilstein J. Nanotechnol. **7** (1), 1141-1155 (2016).